Radial propagation in population dynamics with density-dependent diffusion

Waipot Ngamsaad*

Division of Physics, School of Science, University of Phayao, Mueang Phayao, Phayao 56000, Thailand

(Received 13 May 2013; revised manuscript received 1 November 2013; published 15 January 2014)

Population dynamics that evolve in a radial symmetric geometry are investigated. The nonlinear reaction-diffusion model, which depends on population density, is employed as the governing equation for this system. The approximate analytical solution to this equation is found. It shows that the population density evolves from the initial state and propagates in a traveling-wave-like manner for a long-time scale. If the distance is insufficiently long, the curvature has an ineluctable influence on the density profile and front speed. In comparison, the analytical solution is in agreement with the numerical solution.

DOI: 10.1103/PhysRevE.89.012122 PACS number(s): 02.30.Jr, 82.40.Ck, 87.23.Cc, 87.18.Hf

The growth and dispersal of species in populations undergo density spreading as a traveling-wave front [1]. This phenomenon has been an active research topic for many decades. In a theoretical framework, the dynamics of a population can be modeled as diffusion with reaction processes. The paradigmatic model is known as the Fisher equation [2], which originated as a model for population genetics [1,3–6]. The solution to this equation has demonstrated the propagation as a traveling-wave front in population dynamics [1,2,7]. This equation and its variant have also appeared in various systems, including chemical dynamics [1], nerve pulse propagation [3], flow in porous media [8], combustion theory [3,5,6], wound healing [9,10], tissue engineering [11,12], and bacterial pattern formation [1,13,14].

In the original Fisher model [2], the evolution of the population density $u(\mathbf{r},t)$, at spatial position $\mathbf{r}$ and time t, is governed by the simplest nonlinear reaction-diffusion equation [1,2]. The reaction term is modeled as a logistic law and it describes the growth of population with limited supply. The movement of an individual is modeled as a random walk [15], where the diffusion coefficient is constant. However, the motion of a biological population is not purely random but moves with sense. To remedy this issue, the directed motion model, in which individuals tend to move in the direction of decreasing populations as fast as increasing density, has been proposed [16,17]. The diffusion coefficient in this model depends on the population density [5,6,16–18]. Later, a general form of the logistic law was found [6]. With these modifications, the density-dependent reaction-diffusion equation or the extended Fisher model was presented as [1,5,6,19,20]

$$\frac{\partial u}{\partial t} = \nabla \cdot \left[D\left(\frac{u}{u_M}\right)^p \nabla u \right] + \alpha u \left[1 - \left(\frac{u}{u_M}\right)^p \right], \qquad (1)$$

where $p > 0$, D is the diffusion constant, α is the rate constant, and u_M is the maximum population density.

The solution to Eq. (1) in one dimension (1D) is known as a sharp traveling wave, propagating with a constant front speed [1,5,6,21]. In our previous work, we found a general form of the solution to Eq. (1) in one-dimensional space [20]. This solution shows that the population density evolves, from a specific initial condition, as a self-similar pattern that converges to the traveling wave on a long-time scale [20]. Although the solution to Eq. (1) in one-dimensional space is known [1,5,6,20,21], its behavior in higher dimensions is not well understood. Typically, the population dynamics takes place in 2D, sometimes in 3D. Therefore, the solution of Eq. (1) in dimension higher than one could provide better insight into the dynamics of populations.

In this work we study the population dynamics that evolves with radial symmetric geometry. In this form the system is governed by the extended Fisher equation (1) in an axisymmetric coordinate system. Before describing further, we change the following quantities to be dimensionless: $u' = u/u_M$, $t' = \alpha t$, and $\mathbf{r}' = \sqrt{(p+1)\alpha/D}\mathbf{r}$. Then the radial symmetric extended Fisher equation in dimensionless form is given by

$$\frac{\partial u}{\partial t} = \frac{\partial^2 u^m}{\partial r^2} + \frac{\gamma}{r}\frac{\partial u^m}{\partial r} + u - u^m, \qquad (2)$$

where $m = p + 1$, $r = |\mathbf{r}|$, $0 \leqslant r < \infty$, $\gamma = N - 1$, and N is the dimension. Here the primes are dropped for convenience. Equation (2) recovers dynamics in 1D when $\gamma = 0$. Since the exact solution to Eq. (2) in 1D has been found [20], we focus on its solution in 2D, as well as in 3D.

Equation (2) does not support the traveling-wave solution because of the presence of the gradient term $(\gamma/r)\partial u^m/\partial r$ [1]. It reduces to a one-dimensional problem at $r \to \infty$, which has a planar traveling wave as its solution. Nevertheless, the behavior of this system at a distance that is not so large has been unclear. It has been mentioned that the effects of curvature can make the front propagation in a reaction-diffusion system somewhat different from the planar case [7,22]. Previously, Eq. (2) in cylindrical coordinates was analyzed by the perturbation method [19]; however, the solution is shown over a large distance that yields the usual traveling wave. More recently, the Lie symmetry method has been employed to solve Eq. (2) for $m = 2$ in cylindrical coordinates ($\gamma = 1$) [23]. Although the exact solution has been found, it is another class and does not reflect the density distribution of the population. In this work we adopt a technique similar to that from our previous studies [20,24] to solve for the solution of Eq. (2). We have found the approximate radial symmetric solution for Eq. (2) in the intermediate regime, for which the distance is not so large. The solution explicitly reveals the curvature effect on the spreading of the population of both the density

*waipot.ng@up.ac.th

profile and front speed in this regime. To verify the analytical solution, we have solved Eq. (2) by a numerical method. The numerical result seems to agree with this approximate solution. It confirms the plausibility of our approximate solution being able to describe the intermediate behavior of system.

Before finding the solution in the general case, we first study the asymptotic behavior of Eq. (2) as time goes to infinity. Equation (2) can be viewed as a one-dimensional nonlinear convection-reaction-diffusion equation with the varying drift coefficient γ/r, similar to [25]. The gradient term $(\gamma/r)\partial u^m/\partial r$ in Eq. (2) is large in the vicinity of the front position $R(t)$; otherwise it is small [7]. Thus we change the gradient term to $(\gamma/R)\partial u^m/\partial r$. The drift coefficient becomes small as $R \to \infty$. In contrast, the nonlinear convection-reaction-diffusion equation with constant drift coefficient ν has been analyzed previously [24,26,27]. It was found that the solution in this case, at long times, converges to the sharp traveling front at speed $c = \sqrt{1+(\nu/2)^2} - \nu/2$ [24,26,27]. For the small varying drift coefficient, we assume that the approximate front speed for Eq. (2) can be obtained by setting $\nu = \gamma/R$,

$$c = \sqrt{1+\left(\frac{\gamma}{2R}\right)^2} - \frac{\gamma}{2R}. \tag{3}$$

The front speed (3) approaches 1 as $R \to \infty$, which is equal to the constant front speed of the planar wave [1,5,6,20,21]. If the solution to Eq. (2) exists, it should result in the front speed (3) as the asymptotic behavior.

We now perform the analysis to find the general form of the density profile that propagates at the front speed of Eq. (3). To a good approximation, we rewrite Eq. (2) in the form

$$\frac{\partial u}{\partial t} = \left(\frac{\partial}{\partial r} + \kappa^*\right)\left(\frac{\partial}{\partial r} - \kappa\right)u^m + u + \frac{\partial \kappa}{\partial r}u^m, \tag{4}$$

where

$$\kappa(r) = \sqrt{1+\left(\frac{\gamma}{2r}\right)^2} - \frac{\gamma}{2r}, \tag{5}$$

$$\kappa^*(r) = \sqrt{1+\left(\frac{\gamma}{2r}\right)^2} + \frac{\gamma}{2r}. \tag{6}$$

We note that $\kappa^* - \kappa = \gamma/r$ and $\kappa^*\kappa = 1$. The correction term in Eq. (4), $\partial\kappa/\partial r = \{1-[1+(2r/\gamma)^2]^{-1/2}\}\frac{\gamma}{2r^2}$, approaches $O(1/r^2)$ for $r \gg \gamma/2$ and $1/\gamma + O(r^2)$ for $r \ll \gamma/2$. Fortunately, this correction term behaves well because it decays from $1/\gamma$ to zero as $r \gg 0$. In addition, at $r \ll \gamma/2$, the correction term does not affect the initial state much while $u \ll 1$. Next, we introduce the transformation $d\eta = dr/\kappa$, which can be evaluated to

$$\eta(r) = \kappa r + \frac{\gamma}{2}\ln(\kappa r). \tag{7}$$

With the transformation (7), Eq. (4), by dropping the correction term, becomes

$$\frac{\partial u}{\partial t} = \kappa^{-1}\left(\frac{\partial}{\partial \eta} + 1\right)\kappa^{-1}\left(\frac{\partial}{\partial \eta} - \kappa^2\right)u^m + u. \tag{8}$$

For $r \gg \gamma/2$, we approximate that $\kappa \approx 1 + O(1/r)$. Applying this approximation to Eq. (8), we obtain

$$\frac{\partial u}{\partial t} \approx \frac{\partial^2 u^m}{\partial \eta^2} + u - u^m. \tag{9}$$

Equation (9) is equivalent to Eq. (2) in 1D, but evolving with η as the spatial coordinate.

By adapting the result from Ref. [20], we obtain the solution to Eq. (9),

$$u(r,t) = \frac{\rho e^t}{[\rho^p(e^{pt}-1)+1]^{1/p}} \times\left\{1-\left[\frac{e^{p[\eta(r)-\eta_0]}}{\rho^p(e^{pt}-1)+1}\right]^{1/(p+1)}\right\}^{1/p}, \tag{10}$$

where $\eta_0 = \eta(r_0)$, r_0 is the initial front position, and ρ is the initial density amplitude. By setting $\gamma = 0$, Eq. (10) recovers the solution in 1D [20]. We note that $u(r,t)$ vanishes after the front position for $r \geqslant R(t)$, which will be determined later. As $r \to 0$, we have $\eta \to -\infty$. This causes the density profile at the origin to approach $u(0,t) = \rho e^t/[\rho^p(e^{pt}-1)+1]^{1/p}$, which is actually the solution of

$$\frac{\partial u(0,t)}{\partial t} = u(0,t) - u^m(0,t). \tag{11}$$

This implies no diffusion at the origin.

At a sufficiently long time that $e^{pt'} \gg 1$ and consequently $\rho^p e^{pt'} \gg 1$, we estimate the transition point

$$t' \approx -\ln\rho. \tag{12}$$

For $t \gg t'$, the solution (10) emerges as a pattern in the form of traveling waves

$$\widetilde{u}(r,t) = \{1-[\rho^{-1}e^{[\eta(r)-t-\eta_0]}]^{p/(p+1)}\}^{1/p}. \tag{13}$$

For $r \gg \gamma/2$, we approximate that $\eta(r) \approx r + \frac{\gamma}{2}\ln r$. It is seen that the logarithmic term does not vanish even at large distances, unless $\gamma = 0$. Therefore, Eq. (13) contains an ineluctable curvature term, which can be called curved traveling-wave-like.

The front position can be calculated from Eq. (13) by determining the first position $R(t)$ that density falls to zero or $\widetilde{u}(R,t) = 0$. After evaluating, we obtain an equation for the front position

$$\eta(R) - \eta_0 = t - t'. \tag{14}$$

From Eq. (14) we see that the front position does not simply depend linearly on time as in the one-dimensional case [20]. By differentiating both sides of Eq. (14) with respect to time, we obtain $\frac{\partial\eta(R)}{\partial R}\frac{dR}{dt} = 1$. This allow us to calculate the front speed $c = \frac{dR}{dt}$, that is,

$$c = \left(\frac{\partial\eta(R)}{\partial R}\right)^{-1} = \sqrt{1+\left(\frac{\gamma}{2R}\right)^2} - \frac{\gamma}{2R}. \tag{15}$$

The front speed (15) obtained from this analysis recovers Eq. (3) as expected. Once again, we have seen that the front speed is altered by the curvature as found in other similar systems [7,22]. At sufficiently large distances that $R \gg \gamma/2$, the front speed can be approximated as a constant $c \approx 1$. This

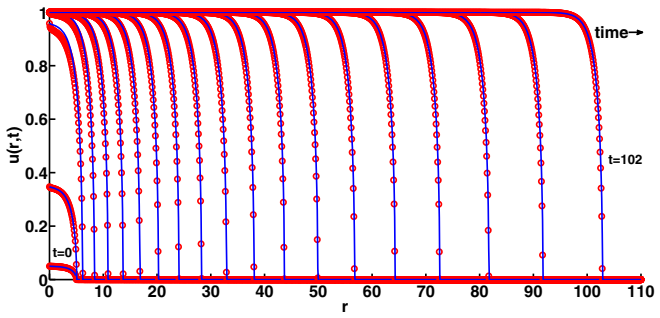

FIG. 1. (Color online) Demonstration of evolution of the radially symmetric population density profile $u(r,t)$ (10) in 2D ($\gamma = 1$) in comparison with the numerical solution. The solid lines represent the exact solutions and the circle markers represent the numerical solutions. The parameters are as follows: $p = 2$, $\rho = 0.05$, and $r_0 = 5$. The density profiles are initiated at $t = 0$ and evolve until $t = 102$.

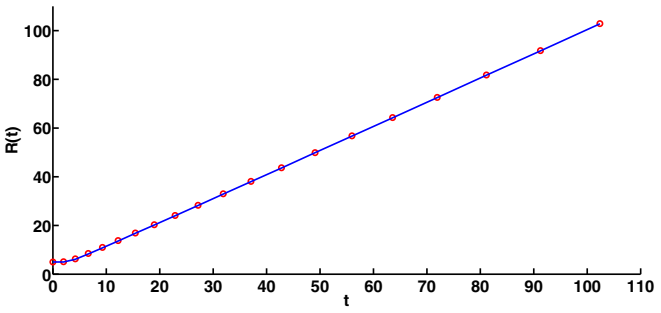

FIG. 2. (Color online) Corresponding front position $R(t)$ extracted from the density profiles in Fig. 1. The solid lines represent the exact solutions and the circle markers represent numerical solutions.

is equal to the front speed in the one-dimensional case ($\gamma = 0$) [1,5,6,20,21].

If we define the quantities $\phi(r) = e^{(p+2)[\eta(r)-\eta_0]/(p+1)}$, $\tau(t) = \rho^p(e^{pt} - 1) + 1$, and $u(r,t) = \rho e^t e^{[\eta(r)-\eta_0]/(p+1)} w(r,t)$, we can rewrite Eq. (10) as the scaling function

$$w(\phi,\tau) = \frac{1}{\tau^\beta} F\left(\frac{\phi}{\tau^\beta}\right), \tag{16}$$

where $\beta = \frac{p+2}{p(p+1)}$, $F(\xi) = [\xi^{-p/(p+2)} - 1]^{1/p}$, and $\xi = \phi/\tau^\beta$. In terms of the transformed density $w(\phi,\tau)$, as a function of transformed space ϕ and time τ, the evolution of the population density in the radial symmetric geometry still holds the self-similarity with the scaling law of Eq. (16). Moreover, this self-similar pattern converges to the traveling-wave-like equation (13) as time becomes long. The connection between the self-similar solution and the traveling wave solution can be described as the intermediate asymptotics of the system [28].

To compare with the analytical solution, we employ the standard explicit finite-difference scheme [29] to solve the radial symmetric extended Fisher equation (2) numerically. Equation (11) is imposed as the boundary condition at the origin ($r = 0$). The boundary condition at the edge of computational domain is free, as the front never reaches this position. The initial density profile for the numerical calculation is set to the same value as the analytical one, $u(r,0)$. The initial front position is chosen such that $r_0 \gg \gamma/2$ since the analytical solution is expected to be accurate at large distances.

The evolution of the population density profiles, obtained from the analytical solution (10) and the numerical solution, is demonstrated in Fig. 1. The density initiates from a sharp profile and then grows locally to a saturated value as it spreads out to an unoccupied region. In the early state, while the density is small, the correction term [the last term in Eq. (4)] does not interfere with the analytical density, as mentioned above. Our approximation is not accurate as the density grows to unity in the early regime. However, it can be seen that both the analytical solution and the numerical solution seem to be in agreement as time and distance become long.

The front position $R(t)$ is also measured directly from the density profiles in Fig. 1. We notice that the small numerical deviation in density can shift the front position from the actual value. Therefore, a density that is less than 10^{-6} can be considered as zero in measuring the front position. A plot of the analytical front position versus numerical front position is shown in Fig. 2. By calculating t for a given measured R, the front position obtained from the density profiles satisfies Eq. (14). Once again, both the analytical front position and the numerical front position are in agreement. We note that, although similar, the data cannot be well fitted to the solution in 1D [20] for a not so large distance.

In summary, we have studied the population dynamics that are described by the density-dependent reaction-diffusion equation, i.e., the so-called the extended Fisher model. We have found the approximate solution to this equation in radial symmetric form in two- and three-dimensional space. The analytical result shows that the evolution of the population density is self-similar. For long-time scales, the population density propagates in a curved traveling-wave-like form. The analytical solutions seem to be in agreement with the numerical solutions. Finally, it was revealed that the density profile and the propagating speed of the evolving population are influenced by the ineluctable curvature at a distance that is insufficiently large.

[1] J. Murray, *Mathematical Biology I: An Introduction* (Springer, New York, 2002).
[2] R. Fisher, Ann. Eugenics **7**, 355 (1937).
[3] D. Aronson and H. Weinberger, in *Partial Differential Equations and Related Topics*, edited by J. A. Goldstein, Vol. 446 (Springer, Berlin, 1975), pp. 5–49.
[4] D. G. Aronson and H. F. Weinberger, Adv. Math. **30**, 33 (1978).
[5] W. Newman, J. Theor. Biol. **85**, 325 (1980).
[6] W. Newman, J. Theor. Biol. **104**, 473 (1983).
[7] V. Volpert and S. Petrovskii, Phys. Life Rev. **6**, 267 (2009).
[8] D. Aronson, in *Nonlinear Diffusion Problems*, edited by A. Fasano and M. Primicerio, Vol. 1224 (Springer, Berlin, 1986), p. 1.
[9] J. A. Sherratt and J. Murray, Proc. R. Soc. London Ser. B **241**, 29 (1990).
[10] P. K. Maini, D. S. McElwain, and D. I. Leavesley, Tissue Eng. **10**, 475 (2004).

[11] B. G. Sengers, C. P. Please, and R. O. Oreffo, J. R. Soc. Interface **4**, 1107 (2007).
[12] M. J. Simpson, K. K. Treloar, B. J. Binder, P. Haridas, K. J. Manton, D. I. Leavesley, D. S. McElwain, and R. E. Baker, J. R. Soc. Interface **10**, 20130007 (2013).
[13] K. Kawasaki, A. Mochizuki, M. Matsushita, T. Umeda, and N. Shigesada, J. Theor. Biol. **188**, 177 (1997).
[14] E. Ben-Jacob, I. Cohen, and H. Levine, Adv. Phys. **49**, 395 (2000).
[15] J. Skellam, Biometrika **38**, 196 (1951).
[16] W. Gurney and R. Nisbet, J. Theor. Biol. **52**, 441 (1975).
[17] W. Gurney and R. Nisbet, J. Theor. Biol. **56**, 249 (1976).
[18] M. Gurtin and R. MacCamy, Math. Biosci. **33**, 35 (1977).
[19] T. P. Witelski, Appl. Math. Lett. **8**, 57 (1995).
[20] W. Ngamsaad and K. Khompurngson, Phys. Rev. E **85**, 066120 (2012).
[21] P. Rosenau, Phys. Rev. Lett. **88**, 194501 (2002).
[22] T. P. Witelski, K. Ono, and T. J. Kaper, Nat. Resour. Model. **13**, 339 (2000).
[23] A. H. Bokhari, M. Mustafa, and F. Zaman, Nonlinear Anal. **69**, 4803 (2008).
[24] W. Ngamsaad and K. Khompurngson, Phys. Rev. E **86**, 062901 (2012).
[25] K. Uchiyama, Arch. Ration. Mech. Anal. **90**, 291 (1985).
[26] B. Gilding and R. Kersner, J. Phys. A: Math. Gen. **38**, 3367 (2005).
[27] M. Mansour, Rep. Math. Phys. **66**, 375 (2010).
[28] G. Barenblatt and Y. Zel'dovich, Annu. Rev. Fluid Mech. **4**, 285 (1972).
[29] W. H. Press, B. P. Flannery, S. A. Teukolsky, and W. T. Vetterling, *Numerical Recipes in C: The Art of Scientific Computing* (Cambridge University Press, Cambridge, 1988).